ISSN 0030-400X, Optics and Spectroscopy, 2020, Vol. 128, No. 5, pp. 582–589. © Pleiades Publishing, Ltd., 2020.

SPECTROSCOPY AND PHYSICS OF ATOMS AND MOLECULES

Structural, Spectroscopic, Electronic Analysis with Nonlinear Optical Activity of L-Methionine L-Methioninium Hydrogen Maleate: A DFT Study

A. Ünal[a, *], M. Okur[b], and Y. Atalay[c]

[a] *Bilecik Şeyh Edebali University, Faculty of Arts and Sciences, Department of Physics, Bilecik, 11210 Turkey*
[b] *Bilecik Şeyh Edebali University, Vocational School of Health Services, Bilecik, 11210 Turkey*
[c] *Sakarya University, Faculty of Arts and Sciences, Department of Physics, Sakarya, 54187 Turkey*
**e-mail: arslan.unal@bilecik.edu.tr*

Received November 13, 2018; revised November 15, 2019; accepted January 31, 2020

Abstract—The molecular structure parameters, vibrational wavenumbers, ^{1}H NMR and ^{13}C NMR chemical shifts of L-methionine L-methioninium hydrogen maleate (LMLMHM) were carried out by using density functional theory (DFT) B3LYP and PBEPBE method using 6-311++G(d,p) basis set. The complete structural analysis such as geometric parameters, vibrational data, NMR chemical shifts of LMLMHM were in good agreement with reported experimental findings. The stability of the molecule arising from charge transfer and hyper-conjugative interaction were researched using natural bonding orbital (NBO), and frontier molecular orbital (FMO) analysis. The electrophilic and nucleophilic sides of the title compound were investigated by using molecular electrostatic potential and Mulliken charge populations. The nonlinear optical features were investigated from the dipole, polarizability and hyperpolarizability values at the same theory levels. The computational finding suggests that mentioned compound has a potential to be used as a nonlinear optical materials.

Keywords: L-methionine L-methioninium hydrogen maleate, density functional theory

DOI: 10.1134/S0030400X20050173

INTRODUCTION

Methionine and its derivatives are generally used in medicinal and industrial applications. A major advantage of methionine moiety in applications is that two sulphur-containing proteinogenic amino acids. Up to now, the researchers have tended to focus on the crystal structure of methionine derivatives or salt complexes [1–3]. A considerable amount of literature has been published on polymer and organic nonlinear optical materials [3–7]. Among recently developed organic molecular and nonlinear crystal materials, stand out in the view of their second order nonlinearity and high laser damage threshold in the pulsed regime. It is interesting to note that the donor and acceptor groups of amino acids are a major influence data on the second order nonlinearity because of providing the ground state charge asymmetry for the related molecule. The result from several studies suggest that amino acids have a pivotal role in nonlinear optical (NLO) applications as they contain a proton donor carboxylic acid (COOH) group and the proton acceptor amino (NH_2) group in them [8–10].

A few study have reported for organic methioninium derivatives about its synthesis and characterization [11–13]. L-Methionine L-methioninium hydrogen maleate (LMLMHM) molecule is synthesized by Natarajan et al. [14] and the crystal form of LMLMHM molecule is experimentally characterized its some thermal and electronic properties by using FT-IR, UV-Vis, and thermal spectroscopies [15]. To the best of our knowledge, quantum chemical calculations investigations for the title compound have not been reported up to now. In the present paper, we aim to model theoretical spectroscopic studies (XRD, IR, and NMR), as well as the NLO and NBO analysis on LMLMHM molecule. Additionally, MEP, FMO energies and molecular charges of LMLMHM are investigated by using quantum chemical calculations.

COMPUTATIONAL DETAILS

The molecular geometry parameters of LMLMHM were fully optimized by using density functional theory (DFT) employing Becke's three-parameter exchange functional in conjunction with the Lee–Yang–Parr correlation functional (B3LYP) [16, 17] and the recommended version of the Perdew–Burke–Ernzerhof functional (PBEPBE) [18] in conjunction with 6-311++G(d,p) basis set [19] without

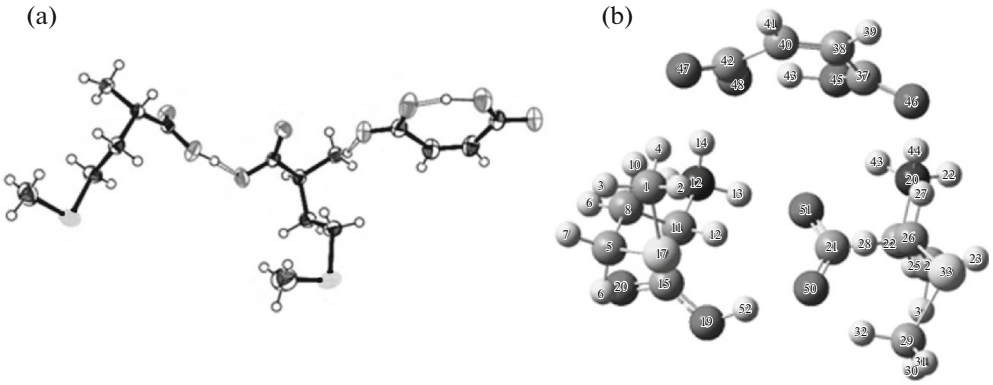

Fig. 1. (a) Experimental [14], (b) optimized molecular structure of L-methionine L-methioninium hydrogen maleate molecule.

any constraint with the help of standard gradient procedure implemented within Gaussian 09W program [20]. All the geometric parameters were allowed to relax and all the calculations converged to an optimized geometry which corresponds to a true energy minimum revealed by the lack of imaginary frequencies in the vibrational mode calculation. The vibrational wavenumbers of LMLMHM molecule were calculated with B3LYP/6-311++G(d,p) and PBEPBE/6-311++G(d,p) levels of theory. The vibrational wavenumbers values, were computed by DFT levels, contain well-known systematic discrepancies. Thus the scaling factor of 0.960 was used for both theory levels in order to repair discrepancies between experimental and theoretical results [21]. DFT theory levels were also used to determine molecular geometric parameters, NMR chemical shifts, NLO, NBO, MEP, FMO, and molecular charges.

RESULTS AND DISCUSSION

Geometrical Structure

The molecular structure parameters of LMLMHM molecule were calculated by using DFT/B3LYP and DFT/PBEPBE levels of theory with 6-311++G(d,p) basis set, and the illustrations of the title molecule are set out in Fig. 1. The title molecule was firstly synthesized by Natarajan et al. [14, 15] and the crystal structure parameters were selected to compare with obtained theoretical results given in Table 1.

The C=O and C–O bond lengths of carboxyl group in methioninium moiety for LMLMHM compound were calculated at 1.319 and 1.209 Å, 1.325 and 1.210 Å by using B3LYP and PBEPBE methods with 6-311++G(d,p) basis set, respectively. These carboxyl group bond lengths were reported at 1.283 and 1.220 Å in the crystal form of title molecule [14, 15]. The carbonyl group bond lengths of methionine residue were obtained at 1.256, 1.270 Å by B3LYP and at 1.266, 1.284 Å by PBEPBE theory level, indicating the double bound character of carbonyl group. The small changes in the carbonyl group bond lengths of methionine and methioninium moieties suggested that these residues were interlinked by a O–H···O intermolecular hydrogen bond. The intermolecular hydrogen bondings were also assumed between maleate anions with both methionine and methioninium moieties. The similar discrepancies at C=O bond lengths of carboxyl group in maleate moiety were supposed due to the N–H...O type intermolecular hydrogen bondings.

Table 1. Molecular structural parameters of LMLMHM molecule

Parameters	Experimental [14]	Theoretical	
		B3LYP	PBEPBE
Bond lengths (Å)			
C13–O19	1.283	1.319	1.325
C13–O20	1.220	1.209	1.210
C11–N18	1.499	1.506	1.507
C21–O51	1.230	1.263	1.273
C21–O50	1.274	1.245	1.256
C22–N36	1.500	1.509	1.510
C42–O48	1.282	1.336	1.340
C42–O47	1.240	1.215	1.228
C37–O46	1.234	1.256	1.266
C37–O45	1.272	1.270	1.284
Bond angles (deg)			
C20–C13–C11	121.86	119.55	119.39
O19–C13–C11	112.00	117.38	117.31
O51–C21–C22	121.41	114.70	115.36
O50–C21–C22	112.81	117.32	116.37
O47–C42–C40	118.70	120.37	119.98
O48–C42–C40	120.00	118.58	118.33
O46–C37–C38	118.40	116.36	116.76
O45–C37–C38	120.00	119.73	120.00

The bond angles O–C–C of maleate residue were calculated in the range of 166° and 120°. Similarly, the related angles in the carboxyl group of methionine and methioninium moiety were obtained circa 117°. When compared to experimental results [14, 15], theoretical methods estimate systematically comparable bond lengths and bond angles.

Vibrational Spectra

The vibration spectra of LMLMHM were simulated to predict the presence of functional groups and their vibrational modes. Vibrational wavenumbers were calculated based on the optimized geometries by using B3LYP and PBEPBE methods with 6-311++G(d,p) basis set. The IR vibration data of LMLMHM are tabulated in Table 2.

The free N–H stretching vibration band appear in 3500–3300 cm^{-1} range [22, 23]. The asymmetric N–H stretching vibrations of methionine and methioninium moieties are assigned in the region 3150–3000 cm^{-1} [6, 15, 22–25]. Hence in the present study the bands at 3310–3105 cm^{-1} (B3LYP) and at 3313–3112 cm^{-1} (PBEPBE) were attributed to asymmetric N–H stretching vibrations. These downward wavenumber shifts in the experimental IR were explained as a weakening of the N–H bonds owing to intra- or inter-molecular hydrogen bondings. The broad medium band at 2918 cm^{-1} is almost certainly due to the asymmetric CH_2–S stretching mode [6, 15, 22–25]. The computed wavenumber for this vibration mode was found at 2932 cm^{-1} for B3LYP and at 2928 cm^{-1} for PBEPBE theory level. The carbonyl stretching wavenumbers normally falls in the range 1760–1660 cm^{-1} for salts of amino acids [6, 15, 26, 27]. When compared with the vibrations of all other group wavenumbers, the peak corresponding to C=O can easily be recognized. The observation of strong bands at 1703 and 1669 cm^{-1} are identified to symmetric stretching of C=O group. These strong band were calculated at 1698 cm^{-1} (B3LYP) and at 1676 cm^{-1} (PBEPBE) theory levels. Similarly, a very strong peak observed at 1572 cm^{-1} and computed at 1564 or 1544 cm^{-1} due to the C–O–O asymmetric stretching. The twin peaks at 1195 and 1182 cm^{-1} are reported to C–O stretching modes for LMLMHM molecule, which were calculated at 1211 and 1209 cm^{-1} (B3LYP) and at 1187 and 1182 cm^{-1} (PBEPBE).

The identification of C–C–N, C–N vibrations are rather difficult since, the mixing of vibrations is possible in this region. However, with the help of the theoretical calculations, these vibrations were identified and assigned easily. The bands at 1115 and 1073 cm^{-1} (B3LYP) and at 1108 and 1069 cm^{-1} (PBEPBE) were assigned to C–C–N and C–N vibrations. These values support the reported results [6, 11–15, 22–29].

Table 2. Selected characteristic vibrational modes for LMLMHM compound

Assignments	Experimental [15]	B3LYP	PBEPBE
$\nu_{as}(NH_3^+)$	3150–3000	3310–3105	3313–3112
ν_{as} (CH_2–S)	2918	2932	2928
ν_{sym} (C=O)	1703, 1669	1698	1676
ν_{as} (COO^-)	1572	1564	1544
ν (C–O)	1195, 1182	1211, 1209	1187, 1182
ν (C–C–N)	1114	1115	1108
ν (C–N)	1066	1073	1069

NMR Spectra

NMR chemical shieldings of LMLMHM were calculated at B3LYP theory level by using GIAO method [30, 31] as implemented in Gaussian 03W program package. The theoretical ^1H and ^{13}C NMR chemical shifts of LMLMHM which are based on the optimized structure were performed by means of B3LYP theory level with 6-311++G(d,p) basis set in water. Isotropic shielding tensors of ^{13}C and ^1H were turned into chemical shifts using the linear relationship equation as in [32]. The experimental proton and carbon NMR chemical shifts of L-methioninium nitrate [33] and L-methionine L-methioninium hydrogen maleate [34] together within the calculated data for LMLMHM in water are given in Table 3.

It is well-known that symmetric C and H atoms in the compounds show the same chemical shift due to having same chemical environment. Considering the chemical environment, LMLMHM compound shows seven different carbon atoms, which is in agreement with the structure regarding the molecular symmetry. The ^{13}C chemical shifts were calculated in the range of 173.74–18.48 ppm for the title molecule. The two carbon signals were clearly calculated for carboxylic groups in the compound at 173.74 and 166.12 ppm. As expected, these chemical shifts are higher than 150 ppm due to the electronegativity features of oxygen atoms. The signals computed at 135.34 and 56.32 ppm were attributed to carbons of two aromatic groups in maleate residue and carbon atoms connected to amino group in L-methionine moiety. Other two signals at 33.12 and 31.56 ppm were assigned to two isopropyl carbons in L-methionine group. The last signal at 16.48 ppm was the methyl group in LMLMHM molecule. All carbons in the compound computed at the expected regions which support the structure of LMLMHM and in accordance with the reported values [15, 33, 34].

^1H chemical shifts from DFT calculation were at the range of 7.81–2.02 ppm. The NMR peak of hydrogen attached or nearby electron withdrawing atom or group appears in the downfield [22]. The proton signals of C–H and C–H_2 groups were determined in the

Table 3. The calculated ^{13}C and ^{1}H NMR chemical shifts (ppm) for LMLMHM in D_2O

Nuclei	Experimental[a, b]	B3LYP/6-311++G(d,p)[c]
C37-21	173.25	173.74
C13-42	170.52	166.12
C38-C40	133.67	135.34
C11-C22	53.08	56.32
C5-C8	29.35	33.12
C24-C26	28.71	31.56
C1-C29	13.90	16.48
H_2-C5-8-24-26	6.26 (2.21–2.11) [b]	2.81–2.34
H_3^+-N18-36	4.14 [b]	7.81
H-C11-22-38-40	3.92–3.89	4.06–3.55
H_3-C1-29	2.03 [b]	2.02

[a]Taken from [34].
[b]Taken from [33].
[c]σ Transform δ into using equations given in [28] $\delta^{13}C = 175.7 - 0.963\sigma^{13}C$ and $\delta^{1}H = 31.0 - 0.970\sigma^{1}H$.

region of 4.06–3.55 and 2.81–2.34 ppm. The signal of methyl group was also calculated at 2.02 ppm. The calculated N–H protons signals (7.81 ppm) shifted towards lower magnetic field by about 3.67 ppm, as compared with reported literature value [35–38]. The rise of this inconsistency should be owing to the solute–solvent interaction, inter- or intra-molecular hydrogen bonding. That's why it is difficult to predict accurately the theoretical NMR signal of N–H proton.

Natural Bonding Orbital Analysis

The natural bonding orbital (NBO) analysis has been a reliable tool for studying intra- and intermolecular bonding and interaction among bonds. It is also used to enable a convenient basis for investigating the charge transfer or conjugative interaction in molecular systems in order to elucidate various second-order interactions between the filled orbitals of one subsystem and vacant orbitals of another subsystem, which are a measure of the intermolecular delocalization or hyperconjugation [39, 40]. The second-order interactions play a critical role in the maintenance of appraise the donor–acceptor interactions in the NBO basis [41]. It is now understood that NBO method plays an important role in examine hyperconjugative interactions due to electron transfers from filled bonding orbitals [42, 43].

The NBO calculations were performed by using B3LYP /6-311++G(d,p) and PBEPBE/6-311++G(d,p) levels. The results from NBO analysis, were tabulated in Table 4, indicated that there were strong hyperconjugative interactions LP3 (O_{51}) → π* (C_{21}–O_{50}) and LP3 (O_{45}) → π*(C_{37}–O_{46}) for the title compound. These interactions have $E(2)$ values calculated as 98.02 and 92.81, 97.86 and 91.11 kcal/mol with B3YLP and PBEPBE theory levels, respectively. The second-order effects in NBO basis showed strong intramolecular hyperconjugative interactions of electrons. These large intramolecular interaction energies are also indicator of the intramolecular charge transfer (ICT). The interaction energies of LP2 (O_{45}) →

Table 4. Second order perturbation theory of Fock matrix in NBO basic corresponding to the intermolecular bonds of LMLMHM molecule

Type	Donor	Type	Acceptor	$E(2)$ (kcal/mol)	
				B3LYP	PBEPBE
LP(2)	O19	π*	C13–O20	52.73	52.09
LP(2)	O20	σ*	C11–C13	19.96	19.82
LP(2)	O20	σ*	C13–O19	27.65	27.42
LP(2)	O50	σ*	O19–H52	32.80	32.42
LP(1)	O51	σ*	H15–N18	10.70	10.57
LP(2)	O51	σ*	H15–N18	26.84	26.45
LP(2)	O50	σ*	C21–C22	18.85	18.24
LP(2)	O50	σ*	C21–O51	12.74	12.02
LP(2)	O51	σ*	C21–C22	16.67	16.46
LP(2)	O51	σ*	C21–O50	10.53	10.02
LP(3)	O51	π*	C21–O50	98.02	97.86
LP(3)	O51	σ*	C21–O51	21.34	21.17
LP(1)	O48	σ*	H14–N18	13.84	13.12
LP(2)	O46	σ*	N36–H44	34.36	34.28
π	C38–C40	π*	C37–O46	11.88	11.91
π	C38–C40	π*	C42–O47	14.98	13.97
LP(2)	O45	σ*	C37–O46	15.99	15.33
LP(2)	O45	σ*	O48–H49	75.13	74.54
LP(3)	O45	π*	C37–O46	92.81	91.11
LP(3)	O45	σ*	O48–H49	19.02	18.40
LP(2)	O46	σ*	C37–C38	14.74	14.84
LP(2)	O46	σ*	C37–O45	11.77	11.49
LP(2)	O47	σ*	C40–C42	17.18	16.98
LP(2)	O47	σ*	C42–O48	28.64	28.40
LP(2)	O48	π*	C42–O47	48.02	47.94
π*	C37–O46	π*	C38–C40	26.06	25.64
π*	C42–O47	π*	C38–C40	38.74	38.44

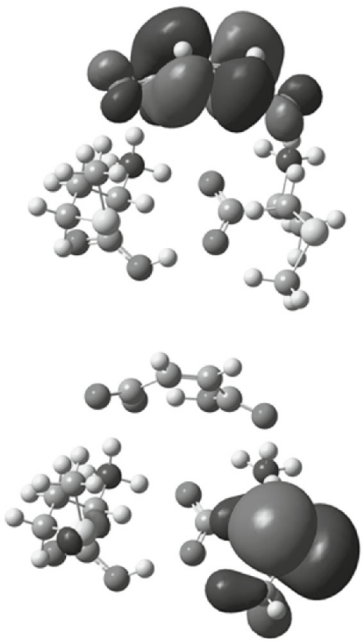

B3LYP	PBEPBE
$E_{LUMO} = -5.476$ eV	$E_{LUMO} = -5.424$ eV
$\Delta E = 1.777$ eV	$\Delta E = 1.841$ eV
$E_{HOMO} = -7.253$ eV	$E_{HOMO} = -7.265$ eV

Fig. 2. The atomic orbital composition of the molecular orbital for LMLMHM molecule.

$\sigma^*(O_{48}–H_{49})$, LP2 $(O_{19}) \rightarrow \pi^*(C_{13}–O_{20})$, and LP2 $(O_{48}) \rightarrow \pi^*(C_{42}–O_{47})$ were calculated as 75.13, 52.73, and 48.02 kcal/mol (B3LYP). The results showed large interaction energy values are indicator of the weakening the respective bonds that causing stabilization of the title compound in ICT. In the same way, the effects of other donor acceptor groups in title molecule can be clearly seen in Table 4.

Frontier Molecular Orbitals

The highest occupied molecular orbital (HOMO) is fundamental to electron donor and the lowest unoccupied molecular orbital (LUMO) is frequently prescribed for electron acceptor, are called frontier molecular orbitals (FMOs). The FMO is an important component in the molecular orbital analysis which plays a key role in electronic devices [44]. The energy gap between HOMO and LUMO (GapHL) characterizes the molecular chemical stability. It is also an essential parameter for determining molecular electrical transport properties or electron conductivity.

The HOMO and LUMO energies of LMLMHM were calculated by using B3LYP/6-311++G(d,p) theory level. From Fig. 2, HOMO and LUMO energies were predicted as –7.253 and –5.476 eV. The GapHL was found as 1.777 eV, and this energy gap showed that the intermolecular charge transfer occur in LMLMHM. Additionally, it is well known that the more HOMO–LUMO energy gap is low, the more charge transportation is possible.

Nonlinear Optical Analysis

There is a growing body of literature that recognizes the importance of intramolecular charge transfer interactions may be responsible for NLO properties. Dipole moment is a common condition which has considerable impact on an indicator of the charge movement across the molecule and this parameter is a dominant feature of designing NLO materials. We investigated the values of the total static dipole moment (μ), the mean polarizability ($\langle\alpha\rangle$), and the mean first-order hyperpolarizability ($\langle\beta\rangle$) which were calculated as in [45].

The dipole moment, mean polarizability and hyperpolarizability values were calculated by using B3LYP and PBEPBE theory levels. The dipole moment, mean polarizability and hyperpolarizability values were obtained as 4.2604 D, 38.8×10^{-24} and 29.1×10^{-30} esu for B3LYP and 4.2586 D, 38.1×10^{-24} and 28.9×10^{-30} esu for PBEPBE. These values, being quite remarkable when compared with literature [42–46], indicate that LMLMHM molecule can be used as an effective NLO material.

Molecular Electrostatic Potential Surface

Molecular electrostatic potential (MEP) has been instrumental in our understanding of the presence of intra- and inter-molecular interactions and there is a growing body of literature that recognizes the importance of the reactive sites and relative reactivities towards electrophilic attack [47]. It also provides a visual method to understand the relative polarity of

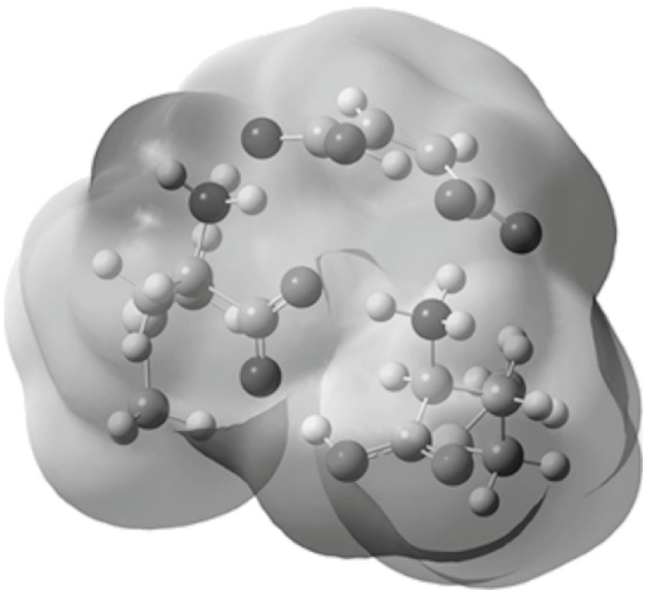

Fig. 3. Molecular electrostatic potential surface for LMLMHM molecule.

the molecule. To predict reactive sites for electrophilic and nucleophilic attack for LMLMHM compound, the MEP is simulated at B3LYP/6-311++G(d,p) theory level. The negative (red and yellow) regions of the MEP are related to electrophilic reactivity while the positive (blue) regions to nucleophilic reactivity [48]. With the more clear expression, the color scheme for the MEP surface is as follows: red for electron rich, partially negative charge; blue for electron decent, partially positive charge; light blue for slightly electron decent region; yellow for slightly electron rich region; green for neutral; respectively [49]. As it can be seen from Fig. 3, negative region is mainly localized over the nitrogen atoms, indicating a possible site for electrophilic attack. The maximum positive region is localized on hydrogens of carboxylic group, indicating a possible site for nucleophilic attack. These sites give information about the region from where the compound can have intermolecular interactions.

Mulliken Charge Analysis

The Mulliken [50] charge distributions of LMLMHM were calculated at B3LYP/6-311++G(d,p) and PBEPBE/6-311++G(d,p) levels of theory. Furthermore, the comparison of Mulliken atomic charges for LMLMHM obtained at B3LYP and PBEPBE theory is given in Fig. 4. As can be seen in Fig. 4, the magnitudes of the carbon Mulliken charges, found to be either positive or negative, was noted to change from –0.95206 to 0.21525 at B3LYP/6-311++G(d,p) and –1.18108 to 0.31732 at PBEPBE/6-311++G(d,p) theory levels, respectively. Carbon atoms bounded to O atoms have more negative charge than other C atoms due to the electronegativity properties of O atom. The whole proton and sulfur atoms have a positive charge, while the oxygen and nitrogen atoms have negative charges. The most positive charge is over S17 atom, while the most negative charge is over C24 atom.

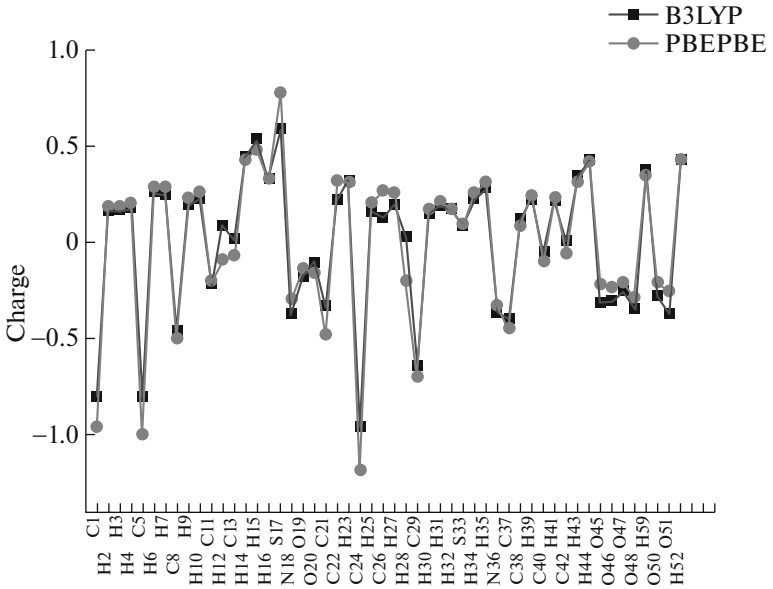

Fig. 4. Mulliken charge distributions plots of LMLMHM compound.

CONCLUSIONS

The structural, spectroscopic, electronic and nonlinear optical properties of L-methionine L-methioninium hydrogen maleate (LMLMHM) are investigated by the application of the B3LYP and PBEPBE levels with the 6-311++G(d,p) basis set. LMLMHM was optimized in ground state by density functional theory levels, and obtained structural parameters are in good agreement with reported XRD results. N–H...O and O–H...O hydrogen bonding interactions are supposed from the small changes of bond lengths and bond angles. The calculated vibration wavenumbers and approximate descriptions of normal modes were investigated by using B3LYP and PBEPBE functional. In IR calculations, the N–H stretching vibration modes appear in different regions of the vibration spectra. This difference is derived from the hydrogen bonding interactions, i.e., the NH vibration mode without the hydrogen bonding interactions appears in high wavenumbers. In other words, hydrogen bonding interactions reduce the wavenumber of the mentioned vibration mode. The vibration peak (C=O, C=N, C=C, O–H, and N–H) moieties may be contribute to the nonlinear optical activity of LMLMHM. ^{1}H and ^{13}C NMR spectra simulated for LMLMHM give results in the expected regions. The reported and the calculated isotropic chemical shifts are found to be in good agreement with the exception of N–H protons shift. The reason of this discrepancy can be shown due to the intra- or inter-molecular hydrogen bonding. These hydrogen bonding interactions are also proved by the NBO analysis. From MEP and Mulliken charges, the electrophilic and nucleophilic regions are demonstrated, and the formation of hydrogen bonding interactions is explained. The energy gap between HOMO and LUMO has been found to be appropriate for charge transfer interactions within LMLMHM. Obtained large α and β values indicate that the LMLMHM compound is a good candidate for nonlinear optical materials.

FUNDING

This work was supported by the Bilecik Şeyh Edebali University Scientific Research Projects Unit, project no. 2017-02.BŞEÜ.04-01.

REFERENCES

1. K. Torii and Y. Iitaka, Acta Crystallogr., B **29**, 2799 (1973).
2. M. Alagar, R. V. Krishnakumar, A. Mostad, and S. Natarajan, Acta Crystallogr., E **61**, o1165 (2005).
3. M. Alagar, M. S. SubhaNandhini, R. V. Krishnakumar, A. Mostad, and S. Natarajan, Acta Crystallogr., E **57**, o396 (2002).
4. K. Rajagopal, R. V. Krishnakumar, A. Mostad, and S. Natarajan, Acta Crystallogr., E **59**, o31 (2003).
5. S. Natarajan, S. A. Martin Britto, and E. Ramachandran, Cryst. Growth Des. **6**, 137 (2006).
6. Y. Shi, C. Zhang, H. Zhang, J. H. Bechatel, L. R. Dalton, B. H. Robinsion, and W. H. Steier, Science (Washington, DC, U. S.) **288**, 119 (2000).
7. F. Kajzar, K. S. Lee, and A. K. Y. Jen, Adv. Polym. Sci. **161**, 1 (2003).
8. T. Pal, T. Kar, G. Bocelli, and L. Rigi, Cryst. Growth Des. **3**, 13 (2003).
9. V. V. Ghazaryan, M. Fleck, and A. M. Petrosyan, Spectrochim. Acta A **142**, 344 (2015).
10. S. Ramaswamy, B. Sridhar, V. Ramakrishnan, and R. K. Rajaram, Acta Crystallogr., E **60**, o1691 (2004).
11. S. A. Martin Britto Dhas, M. Suresh, G. Bhagavannarayana, and S. Natarajan, J. Cryst. Growth **308**, 48 (2007).
12. B. J. M. Rajkumar and V. Ramakrishnan, Spectrochim. Acta A **57**, 247 (2001).
13. K. Anitha, B. Sridhar, and R. K. Rajaram, Acta Crystallogr., E **60**, o1530 (2004).
14. S. Natarajan, N. R. Devi, S. D. M. B. Dhas, and S. Athimoolam, Sci. Technol. Adv. Mater. **9**, 025012 (2008).
15. S. Natarajan, N. R. Devi, S. D. M. B. Dhas, and S. Athimoolam, J. Optoelectron. Adv. Mater. **4**, 516 (2010).
16. A. D. Becke, J. Chem. Phys. **98**, 5648 (1993).
17. C. Lee, W. Yang, and R. G. Parr, Phys. Rev. B **37**, 785 (1988).
18. J. Heyd and G. Scuseria, J. Chem. Phys. **121**, 1187 (2004).
19. M. J. Frisch, J. A. Pople, and J. S. Binkley, J. Chem. Phys. **80**, 3265 (1984).
20. M. J. Frisch et al., *Gaussian 09, Revision A.1* (Gaussian, Inc., Wallingford CT, 2009)
21. A. ünal, M. Senyel, and Ş. Şentürk, Vibr. Spectrosc. **50**, 277 (2009).
22. M. Okur, N. Öner, D. Avcı, Ö. Tamer, and Y. Atalay, Braz. J. Phys. **48**, 398 (2018).
23. Ö. Tamer, D. Avcı, and Y. Atalay, Spectrochim. Acta A **117**, 78 (2014).
24. D. Avcı and Y. Atalay, Int. J. Quantum Chem. **109**, 328 (2009).
25. D. Avcı, Spectrochim. Acta A **82**, 37 (2011).
26. S. Pandiarajan, M. Umadevi, M. Briget Mary, R. K. Rajaram, and V. Ramakrishnan, J. Raman Spectrosc. **35**, 907 (2004).
27. R. M. Silverstein and F. X. Webster, *Spectrometric Identification of Organic Compounds,* 6th ed. (New York, Wiley, 1998).
28. B. Eren and A.Ünal, Spectrochim. Acta A **103**, 222 (2013).
29. N. Öner, Ö. Tamer, D. Avcı, and Y. Atalay, Spectrochim. Acta, Part A **133**, 542 (2014).
30. E. Tarcan, A. Pekparlak, D. Avcı, and Y. Atalay, Arab. J. Sci. Eng. **34**, 55 (2009).
31. L. T. Cheng, W. Tam, S. H. Stevenson, G. R. Meredith, G. Rikken, and S. R. Marder, J. Phys. Chem. **95**, 10631 (1991).

32. A. Ünal and B. Eren, Spectrochim. Acta, Part A **114**, 129 (2013).
33. P. Vasudevan, S. Sankar, and D. Jayaraman, Int. J. Chemtech. Res. **5**, 2018 (2013).
34. P. Vasudevan, S. Sankar, and S. Gokuraj, J. Optoelectron. Adv. Mater. **6**, 1107 (2012).
35. M. Senyel, A. Ünal, and Ö. Alver, C. R. Chim. **12**, 808 (2009).
36. H. Alyar, S. Alyar, A. Ünal, N. Özbek, E. Şahin, and N. Karacan, J. Mol. Struct. **1028**, 116 (2012).
37. H. Alyar, A. Ünal, N. Özbek, S. Alyar, and N. Karacan, Spectrochim. Acta, Part A **91**, 39 (2012).
38. A. Ünal and M. Okur, AIP Conf. Proc. **1815**, 100016 (2017).
39. Ö. Tamer, B. Sarıboğa, İ. Uçar, and O. Büyükgüngör, Spectrochim. Acta A **84**, 168 (2011).
40. F. Weinhold and C. Landis, *Valency and Bonding: A Natural Bond Orbital Donor–Acceptor Perspective* (Cambridge Univ. Press, Cambridge, 2005).
41. A. E. Reed, L. A. Curtiss, and F. Weinhold, Chem. Rev. **88**, 899 (1988).
42. H. Pir, N. Günay, Ö. Tamer, D. Avcı, and Y. Atalay, Spectrochim. Acta, Part A **112**, 331 (2013).
43. H. Pir, N. Günay, Ö. Tamer, D. Avcı, E. Tarcan, and Y. Atalay, Mater. Sci. Poland **31**, 357 (2013).
44. K. Fukui, Science (Washington, DC, U.S.) **218**, 747 (1982).
45. D. Avcı, A. Başoğlu, and Y. Atalay, Int. J. Quantum Chem. **111**, 130 (2011).
46. Ö. Tamer, N. Dege, G. Demirtaş, D. Avcı, Y. Atalay, M. Macit, and S. Şahin, J. Mol. Struct. **1063**, 295 (2014).
47. W. Wenseleers, E. Goovaerts, P. Hepp, M. H. Garcia, P. M. Robalo, A. R. Dias, M. F. M. Piedade, and M. T. Duarte, Chem. Phys. Lett. **367**, 390 (2003).
48. V. Mukherjee, N. P. Singh, and R. A. Yadav, Spectrochim. Acta A **73**, 249 (2009).
49. I. Fleming, *Frontier Orbitals and Organic Chemical Reactions* (Wiley, New York, 1976).
50. R. S. Mulliken, J. Chem. Phys. **23**, 1833 (1955).